Generation and growth of sp^3-bonded domains by visible photon irradiation of graphite

Hiromasa Ohnishi[1,*] and Keiichiro Nasu[1,2]

[1]*Solid State Theory Division, Institute of Materials Structure Science, High Energy Accelerator Research Organization (KEK), 1-1 Oho, Tsukuba 305-0801, Japan*

[2]*Graduate University for Advanced Study and CREST JST, 1-1 Oho, Tsukuba 305-0801, Japan*

(Received 28 April 2009; revised manuscript received 18 June 2009; published 23 July 2009)

We theoretically study possible domain type collective structural changes with interlayer σ bonds and periodic buckling patterns, induced by visible photon irradiation onto graphite. The adiabatic potential-energy surface relevant to the generation and growth of this domain in the multidimensional local distortion coordinates of carbons is clarified by means of the semiempirical Brenner theory. The electronic states at various local minima in this adiabatic potential surface are also calculated, in a good agreement with the observed scanning tunneling microscopy image. We will show that the first diaphite domain can be generated by a few visible photons, and grow up to become various nanosized domains by successive photoexcitations.

DOI: 10.1103/PhysRevB.80.014112 PACS number(s): 64.70.Nd, 73.20.At, 78.67.−n

I. INTRODUCTION

There are a variety of materials, even though they are composed only of carbons, and the differences among them are due to the two types of possible bondings: sp^2 and sp^3. There has been interest in the macroscopically condensed phase of carbons at absolute zero temperature and atmospheric pressure, in which the most stable state is the graphite, characterized by the sp^2 bonds, with the diamond, characterized by the sp^3 bonds, being 0.02 eV/atom higher than the graphite.[1] By the total-energy calculation with the local-density approximation (LDA), the energy barrier between the graphite and the diamond is estimated to be about 0.3–0.4 eV/atom.[2–4] Thus, a macroscopic or tremendous energy is required to realize the direct graphite-diamond conversion. Hence the corresponding real synthesis is the application of a high temperature and a high pressure (3000 °C, 15 GPa),[5,6] or strong x ray.[7,8]

In contrast to this situation, the recent experiment by Kanasaki *et al.*[9] may elucidate a new aspect for this graphite-diamond conversion. After the irradiation of visible photons onto graphite, a nanoscale structural change is detected, and it may come from sp^3-like bonds with the contraction of the interlayer distance. Here we briefly recapitulate the essential experimental aspects: (1) the exciting laser, with an energy of 1.57 eV, should be polarized perpendicular to the graphite layers while the one polarized parallel to the graphite layer gives no effect. It means that only the interlayer charge-transfer excitation can trigger this process. (2) The exciting light should be a femtosecond pulse while the picosecond one gives almost no contribution. It means that only a transient generation of an excited electronic wave packet in the semimetallic continuum can efficiently trigger this process. (3) The process is quite nonlinear but less than the ten-photon process. (4) The scanning tunneling microscopy (STM) measurement shows a nanoscale domain, in which one third of carbons sinks down and the residual two thirds rise up from the layer in each six membered ring. Carbons that have sunk down are expected to form σ bonds between graphite layers, whereby the sp^3-like structure is induced. (5) The resultant domain includes more than 1000 carbons and is stable for more than 10 days at room temperature. The electron-diffraction investigation has been performed by Raman *et al.*[11] They revealed that the interlayer distance after the photoirradiation has contracted up to 1.9 Å from the original 3.35 Å.

From the above experimental facts, a possible mechanism of the present process is as follows:[10] when the femtosecond pulse is irradiated onto graphite, an electron-hole pair, spanning two layers, is generated. This electron-hole pair may be unstable, being easily dissipated into the semimetallic continuum of the graphite as plus and minus carriers. Undoubtedly, this is the most dominant relaxation channel of photogenerated carriers as long as the graphite is a good conductor. However, by a small but finite probability, this electron hole is expected to be bounded with each other, just like exciton, through the interlayer Coulomb attraction. This exciton-like electron-hole pair will be self-localized at a certain point of the layer by contracting the interlayer distance only around it. Thus, a local interlayer σ bond is formed.

This photoinduced phenomenon is quite in contrast to the aforementioned direct graphite-diamond conversion. The unique structure is realized only through the iterative local domain formation by a successive visible photon excitation, to which only a finite and microscopic order of energy is required. The unique domain structure, thus appeared, is not the conventional diamond but an intermediate state between the graphite and the diamond. Hence, we will refer it as "diaphite[12]" hereafter for the convenience of explanation.

The present phenomenon should be clarified by the concept of the photoinduced structural phase transition (PSPT).[13–15] Electrons, just after being excited by lights, are usually in the Franck-Condon state with no lattice motion from the starting ground state. However, they afterward induce a motion of surrounding lattice because of a sudden change in their charge distribution. As a result, the whole system reaches a new state within the excited state as a cooperative phenomenon including these electrons and the lattice.

The present process surely starts from the graphite, and the destination may be the diamond. In between, however, there may be various local minima in the adiabatic potential-energy surface spanned by the multidimensional lattice dis-

tortion coordinates of carbons. Then, in this paper, we will be mainly concerned with the minimal domain; in the sense, it is expected to be the most nearest potential minimum from the starting graphite in this multidimensional potential surface. The growth process of this minimal domain will also be clarified.

The whole process of this PSPT will be a complicated one. Then, in this paper, we will clarify the adiabatic path in generating the minimal (or the first) diaphite domain from the perfect graphite. We will also see several more higher energy domains that can grow up from this first diaphite (FD) domain. We start with the two-layer *AB*-stacking graphite, and the local lattice distortion is introduced for various domain formations. Since the diaphite domain is constantly immersed in the vast semimetallic graphite, we expect that all carbons are almost neutral throughout the deformation process. To theoretically calculate such a diaphite domain in a vastly surrounding graphite, the whole carbon cluster should be as large as possible. In our previous application of the *ab initio* LDA theory,[16,17] the cluster size is limited to around 300 carbons per layer due to the restriction from the computational cost. In that case, it is very difficult to eliminate the cluster size effect. Hence, in this paper, the total energy of the system is estimated by means of the semiempirical Brenner potential,[1] with the cluster that consists of about 10^4 carbons per layer. The electronic states related with the diaphite are also clarified, by means of the tight-binding approximation with the Slater-Koster parametrization.[18]

This paper is organized as follows: in Sec. II, methods of the total energy and electronic state calculations are explained. In Sec. III, the adiabatic path in generating the first diaphite domain is clarified. In Sec. IV, the diaphite domain aggregation process is clarified. In Sec. V, few higher energy states are clarified in connection with the growth process of the first diaphite domain. Finally, in Sec. VI, we make a conclusion.

II. METHOD

Let us clarify the adiabatic potential surface related with domain type collective structural changes by means of the semiempirical Brenner potential.[1] The total binding energy by this method is given as

$$E_{\mathrm{tot}} = \frac{1}{2}\sum_{i,j(\neq i)} \{V_{\mathrm{R}}(r_{ij}) - \bar{B}_{ij} V_{\mathrm{A}}(r_{ij})\} f(r_{ij}), \tag{1}$$

where V_{R} and V_{A} are repulsive and attractive radial two-body pair potentials. While the bond order function $\bar{B}_{ij}$ takes into account the three- or four-body force as a function of the bond angle, and $f(r_{ij})$ is the cutoff function of the force range with the bond length (r_{ij}) between ith and jth carbons. We have adopted the Brenner potential *I* in the original method,[1] which is empirically deduced to reproduce almost all existing experimental and theoretical data of various carbon clusters. In fact, this parametrization well reproduces the binding energy of the graphite and the diamond. We have also estimated the adiabatic barrier between the graphite and the diamond under the uniform transformation condition.[2] It is estimated to be 0.35 eV/atom, which agrees well with the LDA results.[2,4]

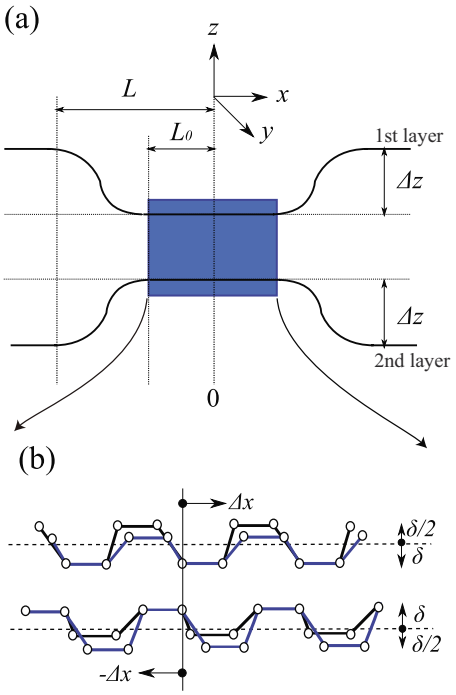

FIG. 1. (Color online) A schematic picture of the trial distortion pattern. (a) The disk type intrusion from the graphite layer. (b) The buckling pattern inside the domain, inferred from the STM image. One third of carbons sink down with the amplitude δ and two thirds of carbons rise up with the amplitude $\delta/2$ in each six membered ring, to keep its center of mass unchanged. Then the total intrusion from the graphite layer is given as $(\Delta z + \delta)$. The local shear displacement is introduced to the opposite direction in each layer. Its value at the domain center is referred to Δx.

To take into account the local domain formation, we have performed the calculation on a large carbon cluster with a two-layer *AB*-stacking structure, consisting of about 10^4 carbons per layer. Although the system does not have the translational symmetry due to the local lattice distortion, we have applied the two-dimensional periodic boundary condition in the directions parallel to the layer. Thus, carbons at around the cluster edge are fixed.

We start from the complete graphite structure with the intralayer bond length 1.42 Å and the interlayer bond length 3.35 Å. The local deformation of the lattice starting from this complete graphite is introduced by taking into account the following displacements: (1) the disk type intrusion from the graphite surface, perpendicular to the graphite layers, with the following trial function for the first layer in Fig. 1 as

$$z = \begin{cases} \bar{z} - \Delta z & (l \le L_0), \\ \bar{z} - \Delta z \dfrac{\tanh[\theta(l-L)] - 1}{\tanh[\theta(L_0 - L)] - 1} & (l > L_0), \end{cases} \tag{2}$$

where $\bar{z}$ is the z coordinate of the original graphite, and $l(=\sqrt{x^2+y^2})$ is the distance from the deformation center in the xy plane. Throughout the simulation, we restrict degrees of

the deformation to keep the total center of the mass of the cluster unchanged. Hence the deformation pattern in the second layer is just the inverse of the first layer against the xy plane at the center of the mass of the cluster. (2) The amplitude $\delta(\geq 0)$ of the buckling: two thirds of carbons rise up, and one third of carbons sink down in each six membered ring, keeping its center of mass unchanged. (3) The local shear displacement $\Delta x(>0)$: each layer is shifted to the opposite direction to improve the interlayer stacking sequence. A schematic picture of this deformation pattern is given in Fig. 1. Here we define the domain as the region that the carbons sunk down more than $\Delta z/2$, and the number of carbons in this domain is referred to as N_d. All the above deformation parameters are variationally determined by systematically changing values.

Electronic states are estimated by means of the tight-binding approximation with the Slater-Koster parametrization.[18] Values of binding energies: ϵ_s and ϵ_p, and hopping integrals: $V_{ss\sigma}$, $V_{sp\sigma}$, $V_{pp\sigma}$, and $V_{pp\pi}$, are used, similar to those in Ref. 17, which are fitted to reproduce the LDA result for the graphite and the diamond. Then, $\epsilon_p-\epsilon_s=8.346$, $V_{ss\sigma}=-4.143$, $V_{sp\sigma}=5.689$, $V_{pp\sigma}=7.758$, and $V_{pp\pi}=-2.489$ in eV unit. The hopping integrals are taken into account up to nearest neighbors, and scaled by the Harrison's r^{-2} rule:[19]

$$V(r) = V(r_0)\left(\frac{r_0}{r}\right)^2, \tag{3}$$

where r_0 is the reference bond length and fixed at 1.54 Å.

III. GENERATION OF THE FIRST DIAPHITE DOMAIN

The adiabatic energy generating the FD domain is clarified. The estimated adiabatic path to this diaphite domain is given in Fig. 2. The energy is referenced from that of the starting complete graphite throughout this paper.

The local minimum, corresponding to the FD, has appeared with the energy 1.700 eV at $L_0=1.878$ Å, $L=2.588$ Å, $\theta=0.20$, $\Delta z=0.75$ Å, $\delta=0.12$ Å, and $\Delta x=0.002$ Å, after overtaking the barrier with an energy of 1.925 eV. Hence the N_d becomes 48 atoms. The averaged interlayer distance becomes 1.85 Å, as shown in Fig. 2(c), which is in a good agreement with the result of the electron-diffraction investigation: 1.9 Å.[11]

The height of the barrier on the FD domain is a little larger than the energy of the irradiated visible light. Then it needs only two or three light quanta to overtake this barrier. We can, thus, conclude that the energy barrier between the starting graphite and the FD can be overtaken by few visible photons. Once the system reaches this FD domain, the structure is well stabilized against the thermal fluctuation at around room temperature. It should be noted that the real process of the generation of the diaphite domain is the Franck-Condon excitation and the lattice relaxation therefrom, as schematically depicted in Fig. 2(b).

The local density of state (LDOS) of this FD is given in Fig. 2(d), together with that of the graphite. This LDOS is calculated at the central carbon site, which forms the interlayer σ bond. Peaks around ± 1 eV have newly appeared only in the case of the diaphite.

The emergence of these peak structures is easily understood from the new bonding between distant graphitic layers. Hence, the system shows the pseudogap, which is characteristic to the insulator immersed in the semimetallic graphite.

IV. DIAPHITE DOMAIN AGGREGATION

Thus, the FD domains may be generated randomly in the graphite surface. They, however, are expected to aggregate or merge afterward into more larger domains during the relaxation.

To clarify these situations, we have estimated the adiabatic energy against the change in the distance between two FD domains. The result is given in Fig. 3. We can consider two aggregating directions due to the periodicity of the diaphite buckling, and those are depicted in right-hand side of Fig. 3. The (a) direction is parallel to the row of carbons that has sunk down from the original graphite surface. The distance between centers of each FD is referred to as R. The calculation has been performed at only R's, which are commensurate with the lattice structure.

At larger R than 34.08 Å, the energy is just twice of the energy of the FD domain because of no mutual interference. While at $R=4.26$ Å, these two domains are completely aggregated, sharing their boundaries. These two situations are separated by a barrier. The height of this barrier is only about 0.07 eV, being sufficiently smaller than the original one for the generation itself [Fig. 2(b)]. Just after the generation of the FD domain, the whole system is still during the lattice relaxation, being not in the equilibrium completely, although it is around the new minimum, which is shown in Fig. 2(b). Hence, during the relaxation, the whole system will overtake the above energy barrier (0.07 eV). Consequently, neighboring two FD domains can easily merge by using the residual energy during the lattice relaxation.

At $R=4.26$ Å, the deformation parameters for the aggregated state along the (a) direction is slightly changed from those of the FD to $\Delta z=0.75$, $\delta=0.14$, and $\Delta x=0.006$. Although this state has a higher energy than the segregated one, this state can also be realized through the aforementioned process. The aggregated state along the (b) direction has the same deformation parameters with the FD. Thus, the FD domain can grow up to become more larger domains.

V. HIGHER ENERGY STATES

In the previous sections, we have clarified the generation of the FD domain, and its naive aggregation process. The estimated FD domain can grow up to become larger domains, passing through various local minima of the adiabatic potential surface by further additional visible photon excitations, and can finally reach the nanosized domain that is observed in the experiment.[9]

In this section, we will theoretically clarify such typical higher energy states by increasing the domain radius (L_0), shown in Fig. 1.

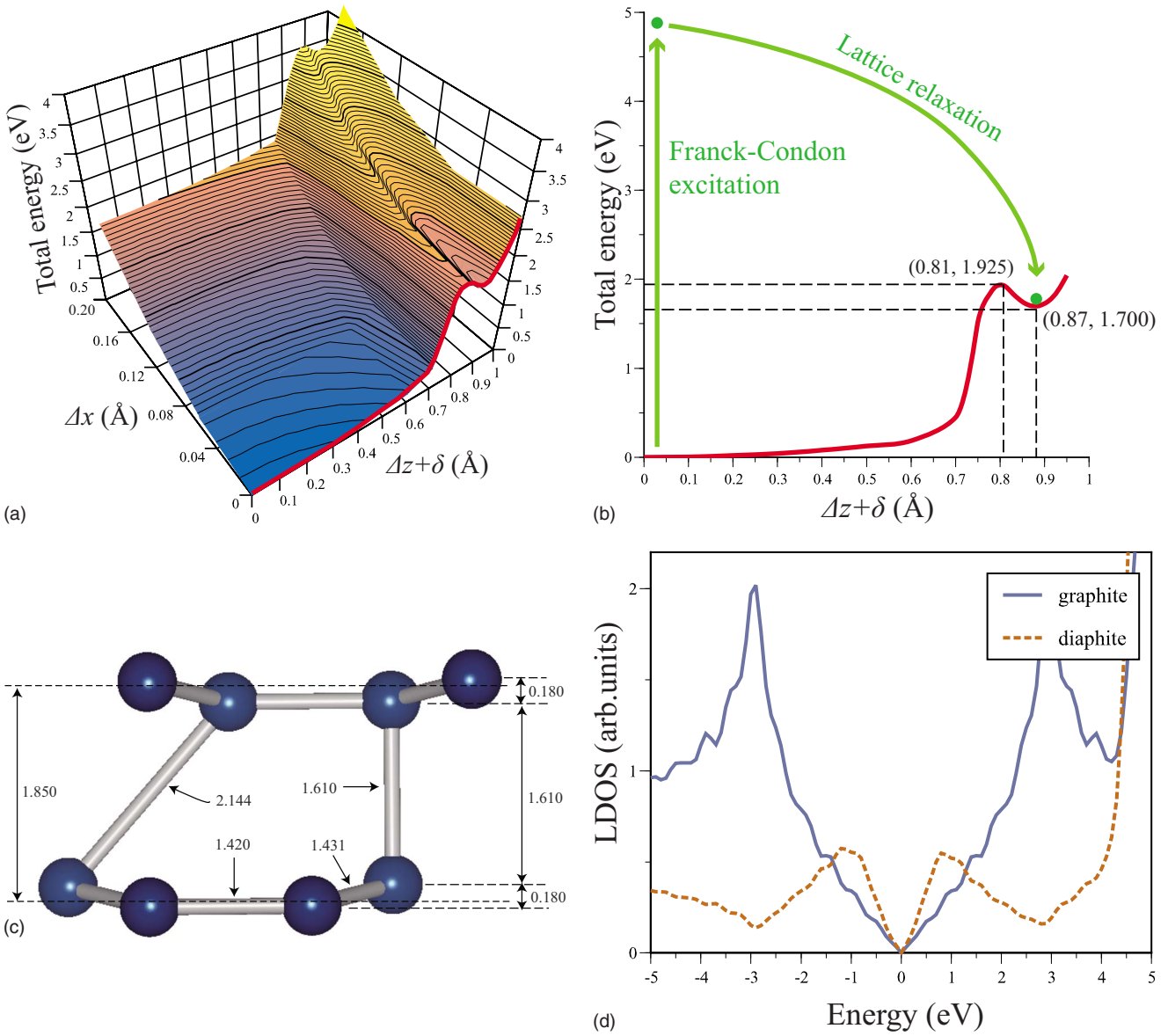

FIG. 2. (Color online) The adiabatic path to the FD. The energy is referenced from that of the starting complete graphite. (a) The adiabatic energy surface as a functional of the total intrusion ($\Delta z+\delta$) and the local shear displacement Δx. (b) The cross sectional view of the adiabatic energy surface at $\Delta x=0.002$, corresponding to the red line in (a). Parenthesized values represent ($\Delta z+\delta$, total energy) at crossing points of dashed lines, respectively. In the real process, the diaphite is realized through the Franck-Condon excitation and the lattice relaxation process therefrom. (c) The estimated diaphite structure. The values are given in angstrom unit (Å). (d) The LDOS of the graphite and the diaphite. The LDOS is calculated at the central carbon site, which forms the interlayer σ bond. The zero of the energy is the Fermi energy of each state.

The calculated higher energy states are summarized in Table I. We have shown four higher energy states, which have different domain radii. Here let us classify them into two groups for the convenience of the explanation. The first group is represented with the symbol (S), which has the large intrusion, $\Delta z=0.75$, and the small buckling amplitude, $\delta \sim 0.2$. The other is represented with symbol (L), which has the relatively small intrusion, $\Delta z \sim 0.5$, and the large buckling amplitude, $\delta=0.40$, compared with the group (S).

The adiabatic path to the (S1) structure from the FD is given in Fig. 4. The (S1) structure with the energy of 10.96 eV at $L_0=5.68$ Å has appeared after overtaking the barrier at $L_0=4.97$ Å with the energy of 11.41 eV along the L_0 direction. Other optimized parameters are given in Table I. Other higher energy states that are given in Table I have also obtained as local minima of the adiabatic potential surface in the multidimensional distortion coordinates although their adiabatic paths are not given.

The states shown in Table I have higher energy than the FD domain. As mentioned before, a tremendous energy will be necessary for the instantaneous generation of such large domains if it will be the conventional uniform phase transition. For example, the energy barrier to the local minimum for the (S1) structure along the ($\Delta z+\delta$) direction is higher than that along the L_0 direction in Fig. 4(a). However, these states will be realized by iterative visible photon excitations

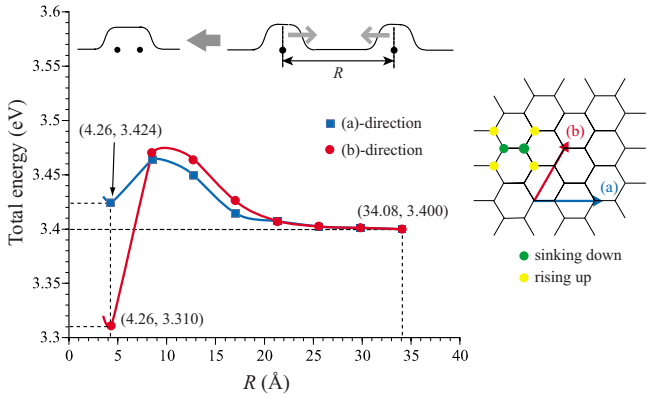

FIG. 3. (Color online) The adiabatic energy against the change in the distance between two FD domains. The parenthesized values represent (R, total energy) at the crossing points of dashed lines. In the top of the figure, the situation is schematically depicted. The approaching directions are represented in the right-hand side of the figure, as the (a) and (b) directions, respectively. The red and yellow circles represent carbons that sink down and rise up, respectively, to indicate the direction of the diaphite buckling.

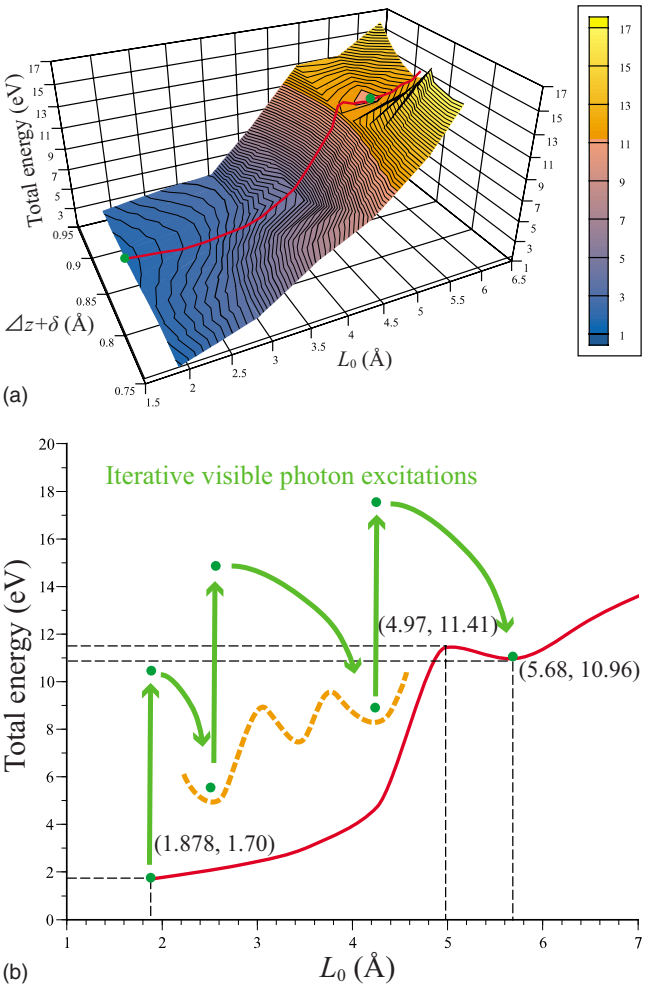

FIG. 4. (Color online) The adiabatic path to the (S1) structure from the FD domain. (a) The adiabatic potential-energy surface as a functional of the L_0 and $(\Delta z+\delta)$. (b) The cross sectional view of the adiabatic energy surface, along the minimal ascending path, corresponding to the red line in (a). The dashed curve schematically represents different valleys that belong to different lattice distortion coordinates. The FD domain will grow up to become a larger domain, only passing through the various local minima of the adiabatic potential surface by iterative visible photon excitations.

from the FD, only passing through the various local minimum of the adiabatic potential surface, as schematically depicted in Fig. 4(b).

The states with larger domain radius take a larger local shear displacement, Δx, in both groups. One can easily infer that the shear displacement makes the interlayer stacking sequence effective since it makes the sp^3 structure more natural. In the present case, however, the shear displacement is introduced in the local region of the lattice, which leads to a stress within a layer, and consequently the system loses the binding energy. Hence, the effectiveness of the local shear displacement is determined by the competition between the increase in the shear stress and the energy gain due to the improvement of the interlayer stacking sequence. The scale of the shear stress within a layer is almost saturated if it is introduced with a sufficiently large radius [$\approx(L+10)$ Å]. The energy gain by the improvement of the interlayer stacking sequence becomes larger and larger according to the increase in the domain radius L_0 because of the increase in interlayer σ bonds. Then, states with large domain radius favor those with large Δx. In the case of the group (S), the structure of each layer is closer to the graphite due to the small buckling. Then, the group (S) needs a large domain radius than the group (L) to overcome the shear stress.

Estimated structures for the (S2) and the (L2) are given in Figs. 5(a) and 5(b), respectively. The averaged interlayer distance for the (S2) becomes 1.85 Å, which is in a good agreement with the experiment[11] structure. The averaged interlayer distance for the (L2) becomes 2.23 Å. Although this value is larger than that of the experiment, the structure is stabilized by the large buckling amplitude. The estimated superstructure of the (L2) type diaphite domain around the domain center is given in Fig. 5(c) as an example. One can

TABLE I. Estimated higher energy states. $E_{\min}$ and E_{top} represent the energy at the local minimum and the barrier top, respectively.

	L_0 (Å)	L (Å)	θ	Δz (Å)	δ (Å)	Δx (Å)	E_{top} (eV)	$E_{\min}$ (eV)	N_d (atom)
(S1)	5.68	6.39	0.22	0.75	0.14	0.01	11.41	10.96	192
(S2)	11.36	12.07	0.40	0.75	0.21	0.27	77.91	77.75	408
(L1)	4.97	5.68	0.30	0.45	0.40	0.02	14.43	13.90	84
(L2)	6.39	7.10	0.20	0.56	0.40	0.22	36.03	30.44	216

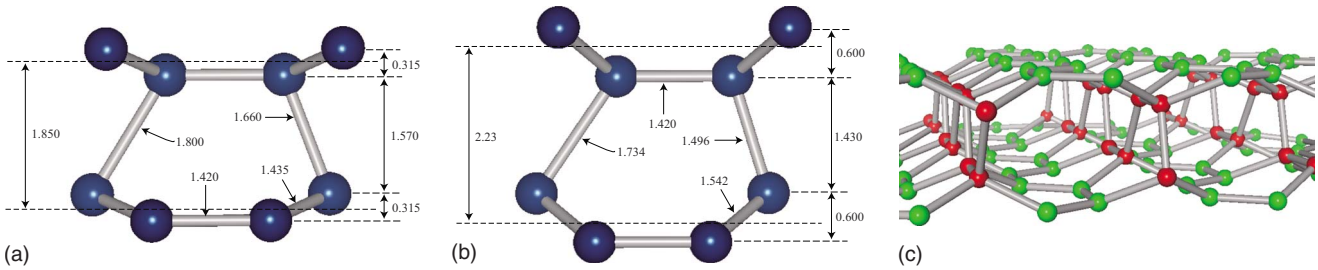

FIG. 5. (Color online) The (a) and (b) represent the estimated structure for the (S2) and the (L2), respectively. The values are given in angstrom unit (Å). The superstructure around the domain center for the (L2) structure is given in (c). The red and green carbons represent the α and β carbons, respectively. The explanation of the α and β carbons is given in the text.

see that the interlayer bonds by the diaphite buckling are formed at the domain center.

The LDOSs for above states are given in Fig. 6. In the diaphite buckling, two types of carbon exist: (a) carbons forming the interlayer σ bonds by sinking down from the distorted layer, referenced as the α carbon. (b) Carbons forming the surface by rising up from the distorted layer, referenced as the β carbon. The LDOSs for the α and β carbons[20] are individually plotted in Fig. 6.

As given in Fig. 6(a), the α carbons in the group (S) show a straightforward opening of the pseudogap according to the increase in the domain radius because the effect of the surrounding semimetallic graphite becomes weaker and weaker with the increase in the domain radius. Although the α carbons in the group (L) also show a pseudogap and its opening, some peak structures have appeared around the Fermi energy. These peak structures can also be seen in the scanning tunneling spectroscopy (STS) measurement,[9] and its origin

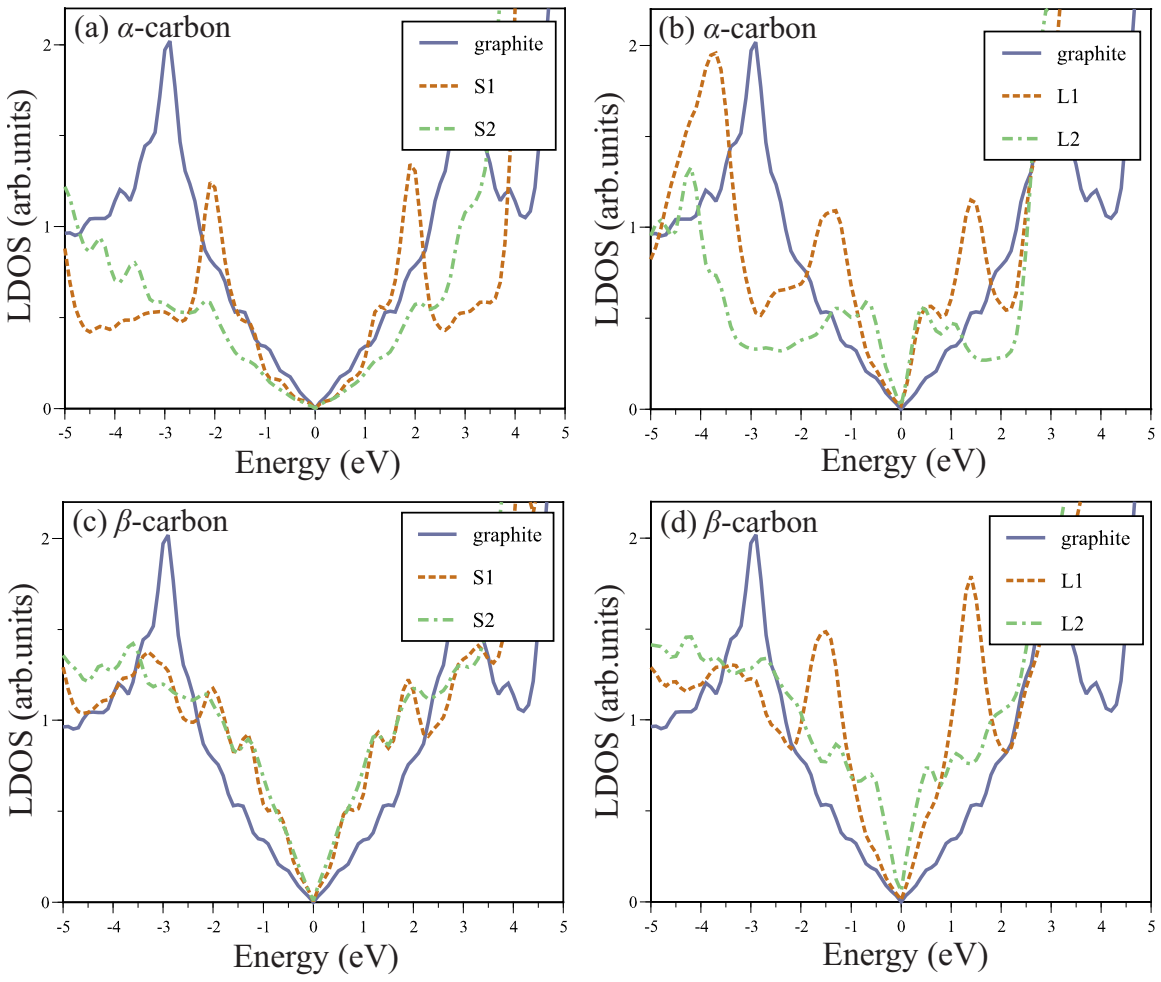

FIG. 6. (Color online) The LDOS for each higher state. The zero of the energy is the Fermi energy of each state. The LDOS of (a) the α carbon for the group (S), (b) the α carbon for the group (L), (c) the β carbon for the group (S), and (d) the β carbon for the group (L), with that of the graphite.

will be argued in connection with the LDOS of the β carbon after a while.

The LDOSs for the β carbons are given in Figs. 6(c) and 6(d). In both groups, the LDOS around the Fermi energy is larger than that of the graphite. This behavior can be understood as follows: the origin of the different LDOSs between the α and β carbons is due to the termination of the sp^3 structure at the surface. Hence, even in the diaphite, surface π bonds still exist. This π bonds are weaker than that of the graphite and will become more weaker according to the stabilization of the sp^3 structure. Then, the LDOS of the β carbons around the Fermi energy is larger than that of the graphite. This behavior of the β carbons can be understood as the origin of the bright STM image of the diaphite domain[9] because the brightness of the STM image is proportional to the surface LDOS of the sample at the Fermi level.[21]

Finally, let us clarify about the LDOS of the α carbons in the group (L). As mentioned above, surface π bonds between β carbons still exist, and its nature is still itinerant just like the graphite. Hence, the α and β carbons are not simply distinguishable, and one can easily find an analogy in the peak structures around the Fermi energy between Figs. 6(b) and 6(d), [and also between Figs. 6(a) and 6(c)]. Then, the peak structures around the Fermi energy are due to itinerant surface π electrons. It should be noted that the origin of the above peak structure is entirely different from that of the FD.

The LDOS of the α carbon of the (L2) diaphite domain is compared with the STS measurement in Fig. 7. The LDOS of the (L2) diaphite domain has shown peaks at around −0.65 and 0.4 eV although the experimental LDOS has peaks at around −0.4 and 0.3 eV. Even though there is such a small difference, the estimated theoretical LDOS well reproduces the characteristics of the experimental result.

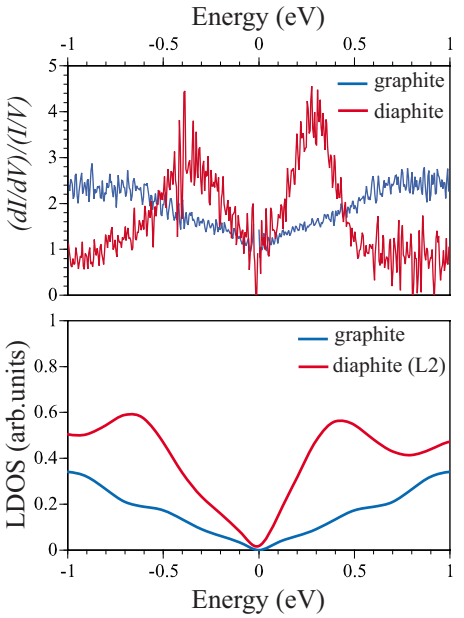

FIG. 7. (Color online) Comparison of the experimental (upper figure) and the theoretical (lower figure) LDOS. The experimental LDOS is obtained by the STS measurement (Ref. 9). The theoretical LDOS is the same as that for the α-carbon of the (L2) diaphite.

VI. CONCLUSION

We have, thus, theoretically clarified the adiabatic path to the diaphite domain from the starting graphite by means of the semiempirical Brenner theory. The FD domain is nucleated by few visible photon excitations, and stable against the thermal fluctuation at around room temperature.

This FD domain can grow up to become various larger domains by further additional visible photon excitations. Along this line, the states with various larger domain radii have also been clarified, wherein the local shear displacement becomes gradually dominant.

Electronic states of diaphite domains have also clarified by means of the tight-binding approximation. The LDOS of them has shown a site-dependent difference between the α and β carbons due to the termination of the diaphite structure at the surface. The behavior of the β carbon can be understood as the origin of the bright STM image of the diaphite domain. The LDOS of the α carbon has shown the pseudogap, characteristic to the insulator immersed in the semimetal. These two orders are closely related to each other, and their origin is the itinerancy of π electrons in the diaphite.

The LDOS of the (L2) structure has well reproduced the experimental one obtained by the STS measurements. Hence, we expect that the diaphite domain, observed in the experiment,[9] have the (L2) type buckling structure.

Thus, we have clarified the generation and growth of the diaphite domain by means of the semiempirical Brenner theory. The present method has led the smaller adiabatic barrier for the generation of the FD domain than our previous result by the LDA calculation.[16,17] In the LDA calculation, it is very difficult to eliminate the cluster size effect, as mentioned before, while the present method can practically treat the infinite size cluster. Although there are such differences, our main conclusion about the generation of the FD domain is not affected by them.

ACKNOWLEDGMENTS

The authors thank K. Tanimura, J. Kanasaki, and E. Inami for presenting their results prior to publication and valuable discussions. This work is supported by the Ministry of Education, Culture, Sports, Science and Technology of Japan, the peta-computing project, and Grant-in-Aid for Scientific Research (S), Contract No. 19001002, 2007.

*ohni@post.kek.jp

[1] D. W. Brenner, Phys. Rev. B **42**, 9458 (1990).
[2] S. Fahy, S. G. Louie, and M. L. Cohen, Phys. Rev. B **34**, 1191 (1986).
[3] S. Fahy, S. G. Louie, and M. L. Cohen, Phys. Rev. B **35**, 7623 (1987).
[4] Y. Tateyama, T. Ogitsu, K. Kusakabe, and S. Tsuneyuki, Phys. Rev. B **54**, 14994 (1996).
[5] F. Bundy, J. Chem. Phys. **38**, 631 (1963).
[6] T. Irifune, A. Kurio, S. Sakamoto, T. Inoue, and H. Sumiya, Nature (London) **421**, 599 (2003).
[7] F. Banhart, J. Appl. Phys. **81**, 3440 (1997).
[8] H. Nakayama and H. Katayama-Yoshida, J. Phys.: Condens. Matter **15**, R1077 (2003).
[9] J. Kanasaki, E. Inami, K. Tanimura, H. Ohnishi, and K. Nasu, Phys. Rev. Lett. **102**, 087402 (2009).
[10] L. Radosinski, K. Nasu, J. Kanazaki, K. Tanimura, A. Radosz, and T. Luty, *Molecular Electronic and Related Materials-Control and Probe with Light*, edited by T. Naito (unpublished).
[11] R. K. Raman, Y. Murooka, C. Y. Ruan, T. Yang, S. Berber, and D. Tománek, Phys. Rev. Lett. **101**, 077401 (2008).
[12] See Research highlight, Nature (London) **458**, 129 (2009).
[13] K. Nasu, *Photo-induced Phase Transitions* (World Scientific, Singapore, 2004).
[14] K. Nasu, Rep. Prog. Phys. **67**, 1607 (2004).
[15] K. Yonemitsu and K. Nasu, Phys. Rep. **465**, 1 (2008).
[16] H. Ohnishi and K. Nasu, J. Phys.: Conf. Ser. **148**, 012059 (2009).
[17] H. Ohnishi and K. Nasu, Phys. Rev. B **79**, 054111 (2009).
[18] J. C. Slater and G. F. Koster, Phys. Rev. **94**, 1498 (1954).
[19] W. A. Harrison, *Electronic Structure and The Properties of Solids (The Physics of The Chemical Bond)* (Dover, New York, 1980).
[20] Note that the present classification of the α and β carbons is different from the often used one, in that the α and β carbons are referred to as carbons having a neighbor in the adjacent layer or not at the surface of the *AB*-stacking graphite, respectively.
[21] J. Tersoff and D. R. Hamann, Phys. Rev. B **31**, 805 (1985).